First Results From the PROBA/CHRIS Hyperspectral/Multiangular Satellite System Over Land and Water Targets

Luis Guanter, Luis Alonso, and José Moreno, *Associate Member, IEEE*

***Abstract*—The Project for On-Board Autonomy (PROBA) platform developed by the European Space Agency was launched on October 22, 2001. The instrument payload includes the Compact High Resolution Imaging Spectrometer (CHRIS). The coupled system provides high spatial resolution hyperspectral/multiangular data, which represents a new-generation source of information for Earth observation purposes. The first results obtained from the preprocessing (noise removal and geometric/atmospheric correction) of two different datasets, collected over agricultural crops and inland waters, are presented in this letter. *In situ* measurements are used to assess the quality of the data and to validate the processing algorithms. The capabilities of this new kind of information for an improved analysis of the surface properties are shown, focusing on the advantages that the coupling between the spectral and the angular domains may have in future Earth observation systems.**

***Index Terms*—Agricultural crops, atmospheric correction, Compact High Resolution Imaging Spectrometer (CHRIS), hyperspectral/multiangular data, inland waters, *in situ* measurements, Project for On-Board Autonomy (PROBA), Spectra Barrax Campaigns (SPARC).**

I. Introduction

THE Project for On-Board Autonomy (PROBA) [1] small-satellite mission launched on October 22, 2001 is a technology-proving experiment to demonstrate the onboard autonomy of a generic platform suitable for small scientific or application missions. Among different sensors, the PROBA payload includes the Compact High Resolution Imaging Spectrometer (CHRIS) [2] instrument.

The PROBA platform provides pointing in both across-track and along-track directions. In this way, the system PROBA/CHRIS has multiangular capabilities, acquiring up to five consecutive images from five different view angles [1] during a single orbital overpass. Typical time differences in the acquisition of the five images are around 3 min. CHRIS measures in the visible/near-infrared (NIR) bands from 400–1050 nm, with a minimum spectral sampling interval ranging between 1.25 (at 400 nm) and 11 nm (at 1000 nm). It can operate in different modes, compromising the number of spectral bands and the spatial resolution because of storage capabilities. For instance, Mode-1 works with 62 spectral bands at a spatial resolution of 34 m, while Mode-2, used for water bodies studies, presents 18 bands at 17 m. As a result, the coupled PROBA/CHRIS system provides information of the target in both the angular and the spectral domains, by means of five observation angles and up to 62 spectral channels. CHRIS images have an approximate swath of 15 km.

The results of the preprocessing (noise removal and geometric/atmospheric correction) for two 2004 PROBA/CHRIS datasets are presented in this letter. To cover a wide range of natural surfaces (horizontally homogeneous and vertically structured green canopies, harvested vegetation crops, dry bare soils, water reservoirs, etc.), two different PROBA/CHRIS sites have been selected: Barrax, which is a midlatitude agricultural area, and Rosarito, an inland waters study site. The main emphasis is put on the analysis of the atmospherically corrected images, discussing the benefits that simultaneous hyperspectral and multiangular information may have in the characterization of the observed targets. Thus, detailed descriptions of the algorithms used in the preprocessing steps will be given in separate papers.

II. PROBA/CHRIS Data Processing

A. Processed Datasets

The main data source has been the two Spectra Barrax Campaigns (SPARC) [3] held in Barrax (39.05°N, 2.10°W, La Mancha, Spain) in July 2003 and 2004, as part of the Phase-A preparations for the Surface Processes and Ecosystem Changes Through Response Analysis (SPECTRA) [4] mission. The Barrax site is a flat continental area with an average elevation over the sea level of around 700 m. There is a big contrast in natural surfaces, ranging from dense green vegetation fields (e.g., alfalfa and potato crops) to dry bare soils, leading to a wide range of leaf area index (LAI), from 0 up to 6.3. All the crops in the site have been classified previously, and many *in situ* measurements were made during the campaign simultaneously to the images acquisition, so field spectra are available for intercomparison and validation of the remote sensing products.

For the sake of simplicity, and due to the claimed better geometrical quality of 2004 data, we shall focus on SPARC 2004. The results presented in this work have been elaborated with the set of five images acquired on July 16, 2004. This dataset is considered sufficient to show the potential of PROBA/CHRIS data for capturing spectral and angular trends expected in agricultural areas.

Manuscript received December 3, 2004; revised April 12, 2005. This work was supported by the European Space Agency under Contract ESTEC-18307/04/NL/FF in the frame of the ESA-SPARC Project.

The authors are with the University of Valencia, 46100 Burjassot-Valencia, Spain (e-mail: luis.guanter@uv.es).

Digital Object Identifier 10.1109/LGRS.2005.851542

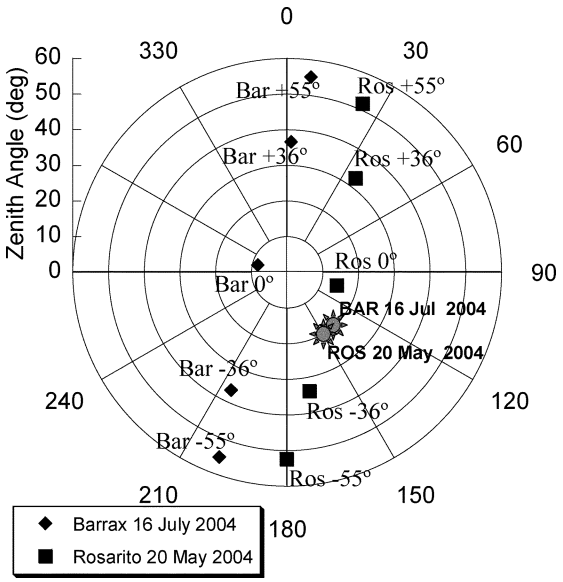

Fig. 1. Acquisition geometries and illumination angles for the images of Barrax (July 16, 2004) and Rosarito (May 20, 2004). Labels indicate the corresponding nominal fly-by zenith Angles.

In addition, PROBA/CHRIS images over inland waters targets have also been processed, in order to assess the information that hyperspectral/multiangular information may provide for water bodies. One Mode-2 image acquired on May 20, 2004 over the Rosarito reservoir, located in Northern Spain (40.12°N, 5.27°W), is presented here. Again, *in situ* measurements are used to validate the results obtained from the processing. The acquisition angles for the Barrax July 16, 2004 and the Rosarito May 20, 2004 images are plotted in Fig. 1.

B. Methodology

Before the derivation of the final surface reflectance product, two processing steps are needed: the removal of horizontal (drop-outs) and vertical (striping) noises and the correction of atmospheric effects. The procedure for the noise removal is based on statistical analysis of the images. A detailed explanation is given in [5].

Concerning the atmospheric correction, only a short overview is given here. Since this letter is intended to be a quick communication of the first results obtained from PROBA/CHRIS data, a schematic description of the algorithm implemented is presented, leaving a more comprehensive version covering all of the details for a future dedicatedpaper.

Since the PROBA/CHRIS system was designed as a technology demonstrator, radiometric performance is somehow limited for scientific applications. For this reason, PROBA/CHRIS 2003 and 2004 data (improvements for 2005 are foreseen [6]) present some miscalibration trends all over the covered spectral region [2], being the underestimation of the signal in the NIR wavelengths the most important one. With this framework, a dedicated atmospheric correction algorithm for PROBA/CHRIS data has been designed. The idea is to derive the appropriate atmospheric parameters and a set of correction factors for CHRIS's gain coefficients altogether.

The procedure starts with the inversion of top-of-atmosphere (TOA) radiances in five pixels extracted from the image acquired with a minimum view zenith angle (VZA). This gives as a result rough estimations of aerosol optical thickness (AOT) and water vapor content, as well as the updated calibration coefficients. All of these variables are used to derive the surface reflectance image afterward. The estimation of the atmospheric parameters is based on the assumption that the atmospheric state is invariant within the CHRIS image, what is justified by the fact that PROBA/CHRIS images are of around 15 km in size. Surface reflectance is modeled as a linear combination of two vegetation and soil spectra, which act as artificial endmembers, with two independent coefficients weighting vegetation and soil proportions. The frequent strategy of using dark targets in the aerosol retrieval is avoided with this approach. It makes the algorithm applicable to any kind of land target, as long as some areas with vegetation and bare soil are present in the window inside the image, which is less restrictive than the dark-targets approach [7].

Several initial analysis led to the choice of five as an optimal number of reference pixels, compromising the computational load and the information content. With the aim of discriminating the contribution of the radiative transfer effects from surface and atmosphere to the TOA radiances registered by the sensor, reference pixels with a maximum spectral contrast (i.e., from the purest vegetation pixels to the purest bare soil ones, with the others being intermediate cases) are extracted from the minimum VZA. The selection is made automatically from dynamic thresholds of the normalized differences vegetation index (NDVI) [8], which may be varied during the process if any of the categories resulted empty.

The TOA radiances in these five reference pixels are inverted, the inversion parameters being the AOT at 550 nm accounting for the aerosol loading, the percentages of four basic types (dust-like, water soluble, oceanic, and soot) for the spectral behavior, the water vapor column content, and the ten coefficients for the proportions of vegetation and soil within the five pixels. They are calculated simultaneously by means of the minimization of a merit function specifically designed, summing the TOA radiances in the whole spectral domain for the five pixels. However, from a previous knowledge on CHRIS performance, channels with wavelengths larger than 940 nm are discarded in the computation of the merit function because of calibration problems. Bands contaminated by ozone (around 500 nm) and oxygen (around 760 nm) absorptions are also avoided in the inversion, as they might perturb the estimation of aerosol and water vapor contents.

From the outputs, the five pairs of real/modeled radiance spectra obtained from the inversion procedure are used for the calculation of the calibration coefficients, by means of linear regressions calculated for each spectral band for the five pixels. The high spectral contrast in the reference pixels ensures the required sampling for the regressions. Once the updated set of gain coefficients is derived, the calculated abundances of aerosols and water vapor are used as an input for the calculation of the atmospheric transmittance and reflectance functions to be applied in the atmospheric correction of the five PROBA/CHRIS images acquired during the same overpass.

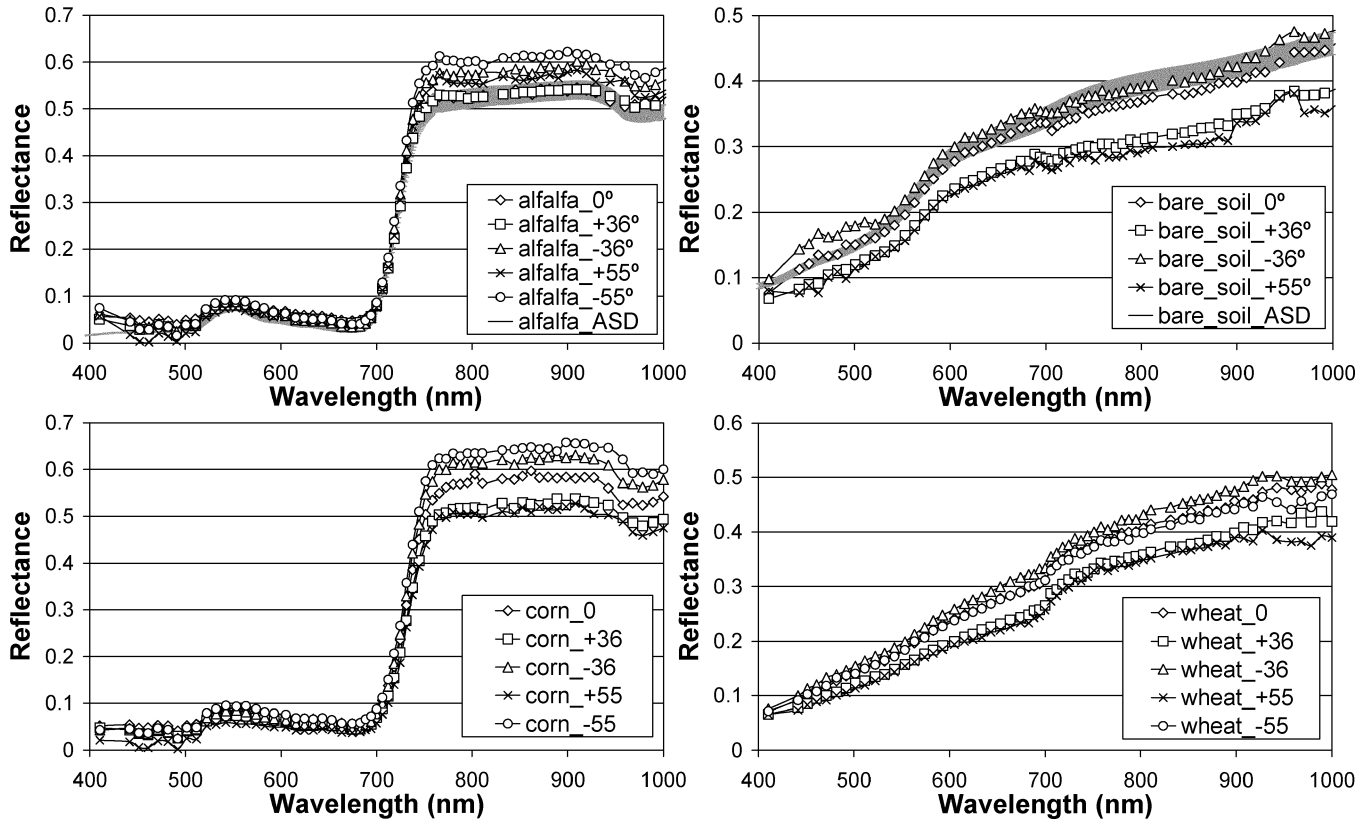

Fig. 2. Sample surface reflectance spectra extracted from the five view angles of Barrax July 16, 2004 images for four different surfaces. Angles in the legends correspond to the view zenith and azimuth angles plotted in Fig. 1. Ground-truth from *in situ* measurements is also plotted for alfalfa and bare soil targets, by a gray stripe giving the mean value and the standard deviation in the measurements.

A final step concerning the correction of adjacency effects is performed.

Since the use of land pixels should be avoided for Mode-2 data [6], due to saturation for surface albedos higher than around 25%, a different approach is followed in the estimation of aerosol loading for water targets. The main idea is to perform an iterative procedure that seeks for the AOT that minimizes the subsequent water reflectance in CHRIS bands 2 and 3 (centered around 440 and 490 nm), where the aerosol scattering is maximal, with the physical constraint that the reflectance has to be positive. Neglecting water vapor variations is not a critical issue, since Mode-2 channels are located in wavelengths out of water vapor absorptions. The use of the first band, centered in 410 nm, is avoided because of the high noise levels detected. No recalibration procedure is needed for this Mode-2: because the signal-to-noise ratio is low in the NIR bands, no miscalibration can be detected in them. Besides, for this reason, the bands in this spectral region are seldom used in water studies.

C. Results

1) Barrax Data: A sample of surface reflectance spectra from the Barrax site is displayed in Fig. 2. They have been manually extracted from the same targets in the five-angle images. *In situ* measurements taken with an Analytical Spectral Devices (ASD) FieldSpect Pro FR Spectroradiometer (footprint around 0.8 m, 2-nm spectral resolution) are also plotted for the alfalfa and bare soil surfaces. These measurements were acquired almost simultaneously to satellite overpasses (time differences were always smaller than 30 min) from a nadir view while walking across the target, integrating in one spectrum all the measurements taken for every path of around 10 m. The reason for this is to ensure that most of the natural variability in the target could be reproduced. In any case, uniformity was one of the criteria followed in the selection of these targets, to minimize the discrepancies arisen in the comparison of instruments with very different footprints. The gray stripe gives the mean value and the standard deviation calculated from all the acquisitions made for the same target, to provide information on the spatial variability of the target.

The agreement between the ASD spectroradiometer and CHRIS data is quite high, both in the shape and in the reflectance levels, which validates the techniques used in the preprocessing of the data. Mean relative and absolute errors have been calculated for bands in the red (ten bands, from 604–688 nm) and in the NIR (ten bands, from 804–900 nm) spectral regions. For the comparison, the *in situ* spectra measured with the ASD were convolved to CHRIS nominal bands configuration. Concerning PROBA/CHRIS spectra, these were extracted from the image acquired from the minimum VZA, labeled by "0" in Fig. 1, which is the closest one to the vertical view used for the field measurement. The mean relative error for the bare soil target is 1.6% in the red and 5.9% in the NIR, while for the alfalfa crop is 77.0% in the red wavelengths, and 0.7% in the NIR ones. The reason for such a large relative error in the red is the low reflectance caused by chlorophyll absorption. However, the absolute error in reflectance is around 0.023

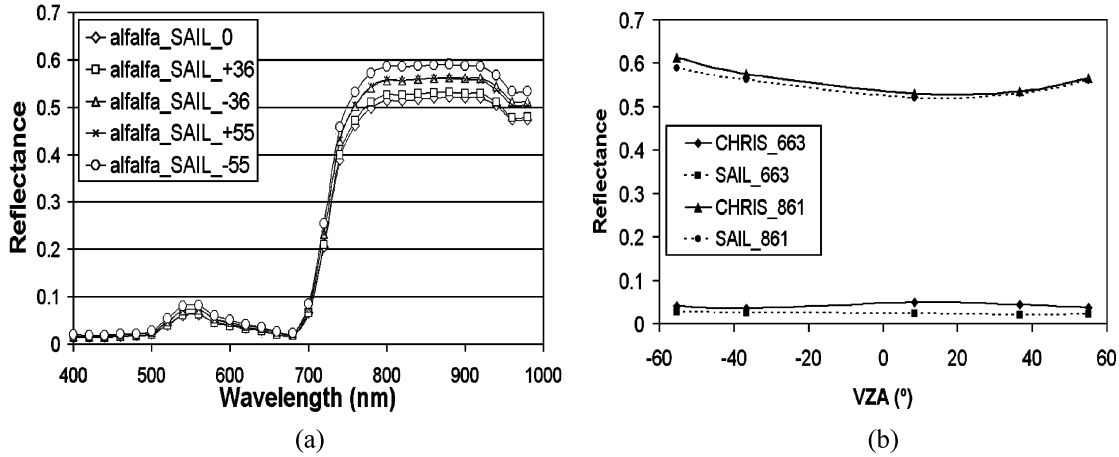

Fig. 3. (a) Results of SAIL/PROSPECT simulations using *in situ* measurements of the biological parameters for the alfalfa crop and the geometrical configuration plotted in Fig. 1. (b) Projection of the alfalfa simulations in (a) on the VZA, for two wavelengths in the red (663 nm) and in the NIR (861 nm) regions.

(normalized to unit), which can be considered small enough for the later use of the data. It must be taken into account that the field spectra were acquired from a nadir view, not coincident with any of the PROBA view angles, so small deviations due to angular trends are expected *a priori*. This is confirmed by the fact that the maximum agreement with the *in situ* measurements is found for the minimum VZA.

It can be stated that the magnitude of the directional effects varies with the nature and vertical structure of the target, according to the behavior predicted by radiative transfer theory. In order to quantify those angular differences, a function δ_i is defined as the standard deviation of the surface reflectance in the five angles for the i channel, normalized by the mean value. The expected dependence on the three-dimensional structure of the canopies is found: the alfalfa crop, consisting of uniform dense short canopies, is closer to the Lambertian behavior than the vertical tall (around 2 m height) corn canopy, where the angular effects are more important. Calculating the mean values of δ for the same two spectral regions used before, we obtain $\delta_{\rm red} = 0.10$ and $\delta_{\rm NIR} = 0.06$ for the alfalfa field, while $\delta_{\rm red} = 0.16$, $\delta_{\rm NIR} = 0.10$ for the corn field. Something similar occurs between the bare soil and the dry wheat targets: although the spectral response is quite similar, directional effects are more intense in bare soils, as the wheat cover consists of a very dense canopy, almost uniform, that tends to make isotropic the angular response due to multiple scattering processes ($\delta_{\rm red} = 0.10$ and $\delta_{\rm NIR} = 0.09$ for the wheat target, while $\delta_{\rm red} = 0.13$, $\delta_{\rm NIR} = 0.14$ for the soil target).

Further validation of the angular trends shown by the alfalfa crop has been achieved using a newer coupled version of the SAIL and PROSPECT models [9]. We have only selected the alfalfa crop for its 2-D uniformity, which makes it the prototype of a crop to be modeled with the SAIL/PROSPECT model. Besides, all the inputs needed (chlorophyll content, LAI, water content, and dry matter content) were explicitly measured during the SPARC 2004 campaign. Results for the five angles in Fig. 1 are plotted in Fig. 3. It can be stated that both the spectral shape [Fig. 3(a)] and the angular dependencies [Fig. 3(b)] are highly coincident with those showed for the alfalfa crop in Fig. 2, what confirms the validity of the procedure applied in the preprocessing of the PROBA/CHRIS data.

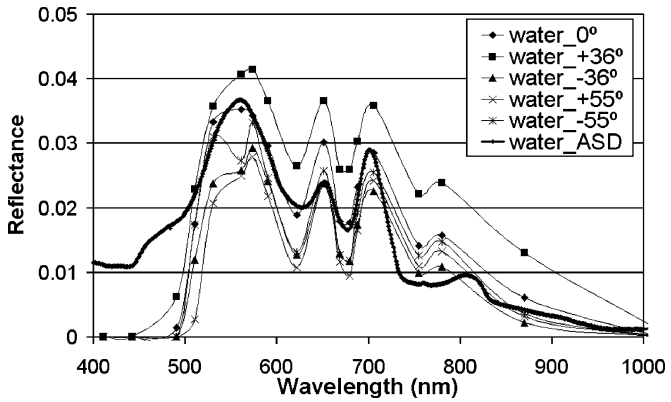

Fig. 4. Comparison of CHRIS water reflectance spectra for the five different observation angles plotted in Fig. 1 with an *in situ* measurement acquired simultaneously on May 20, 2004.

2) Rosarito Data: Results obtained from the atmospheric correction of the Rosarito data of May 20, 2004 are shown in Fig. 4. The five views of the same point in the Rosarito reservoir and the corresponding *in situ* reflectance spectrum measured simultaneously to the PROBA/CHRIS acquisition are plotted. *In situ* measurements come from the Spanish Center for Hydrographic Studies (CEDEX), in the frame of its activities to validate algorithms for the monitoring of water quality using remote sensing data [10].

It has to be remarked the relatively high agreement between CHRIS data and the *in situ* spectrum, taking into account the low signal arriving at the sensor from water targets and that the field measurement angle is not coincident with any of the PROBA/CHRIS observation angles. Nevertheless, the closest spectrum to the nadir-ASD measurement is again corresponding to the minimum VZA, as expected. This validates both the quality of CHRIS Mode-2 data and the aerosol retrieval and atmospheric correction procedures implemented for inland waters.

On the other hand, the large directional behavior expected for water bodies is found in PROBA/CHRIS data: even though ac-

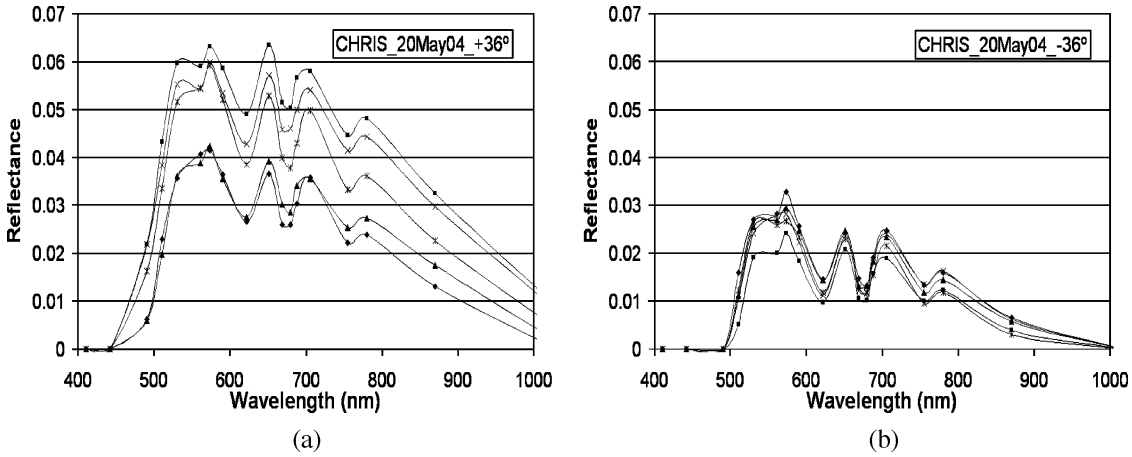

Fig. 5. Sample of Rosarito reflectance spectra, extracted randomly for different pixels across the image, for two different observation angles.

quisition angles are not in the principal solar plane, forward and backward scattering regions can be clearly predicted in Fig. 1. The maximum reflectance should be expected in the specular reflection region, typical in polished surfaces such as calm water bodies. The closest angle to the ideal specular position in the geometrical configuration of the Rosarito scene of May 20, 2004 is the one labeled by "+36." The maximum of reflectance for this angle can be observed in Fig. 4.

Moreover, the angular dependency of the registered reflectance can be found not only in the mean reflectance value, but also in the composition variability inside the reservoir. While the Rosarito reservoir looks very uniform when viewed from one direction, noticeable structures with different tonalities can be seen when it is observed from another one. An example is displayed in Fig. 5, for the "+36" and "−36" angles. Several spectra have been extracted randomly from all over the reservoir. Large differences can be detected in the "+36" angle, while the "−36" appears as much more uniform. Therefore, one observation angle may turn out to be more useful than the other with the aim of water quality analysis. Besides, multiangular information is very useful in the substitution of those pixels mostly affected by the sunglint effect in any of the observation angles.

III. Discussion

First results obtained from data acquired by the new PROBA/CHRIS satellite system have been presented. The processing has involved the noise removal and the atmospheric correction of IMAGES of two different targets, agricultural areas and inland waters, acquired in Mode-1 (vegetation) and Mode-2 (water) CHRIS operation modes.

The capabilities of such hyperspectral/multiangular data in the study of surface features have been outlined, by means of the different spectral and angular responses of the analyzed targets. The spectral signatures of different crops have been properly retrieved, as it was shown by the comparison against *in situ* reflectance measurements, while the observed directional behaviors match with the corresponding theoretical predictions. This confirms the quality of both the PROBA/CHRIS data and the processing algorithms that are currently being developed and validated.

Acknowledgment

L. Guanter acknowledges the support by a Ph.D. grant from the Spanish Government. The authors also want to thank M. Cutter (Sira Technology, Ltd.) and to R. Peña, J. A. Domínguez, and A. Verdú for the provision of inland waters data.

References

[1] M. J. Barnsley, J. J. Settle, M. Cutter, D. Lobb, and F. Teston, "The PROBA/CHRIS mission: A low-cost smallsat for hyperspectral, multiangle, observations of the Earth surface and atmosphere," *IEEE Trans. Geosci. Remote Sens.*, vol. 42, no. 7, pp. 1512–1520, Jul. 2004.

[2] M. Cutter, "Review of aspects associated with the chris calibration," presented at the *2nd CHRIS/PROBA Workshop*, Frascati, Italy, Apr. 2004.

[3] J. Moreno *et al.*, "The SPECTRA Barrax Campaign (SPARC): Overview and first results from CHRIS data," presented at the *2nd CHRIS/PROBA Workshop*, Frascati, Italy, Apr. 2004.

[4] M. Rast, "SPECTRA—Surface Processes and Ecosystem Changes Through Response Analysis,", Noordwijk, The Netherlands, ESA SP-1279(2), 2004.

[5] J. C. García and J. Moreno, "Removal of noises in CHRIS/PROBA images: Application to the SPARC campaign data," presented at the *2nd CHRIS/PROBA Workshop*, Frascati, Italy, Apr. 2004.

[6] M. Cutter, private communication, 2004.

[7] Y. J. Kaufman and C. Sendra, "Algorithm for atmospheric corrections," *Int. J. Remote Sens.*, vol. 9, pp. 1357–1381, 1988.

[8] C. O. Justice, J. G. R. Townshend, B. N. Holben, and C. J. Tucker, "Analysis of the phenology of global vegetation using meteorological satellite data," *Int. J. Remote Sens.*, vol. 6, pp. 1271–1318, 1985.

[9] J. R. Miller, M. Berger, L. Alonso, Z. Cerovic, Y. Goulas, S. Jacquemoud, J. Louis, G. Mohammed, I. Moya, R. Pedros, J. F. Moreno, W. Verhoef, and P. J. Zarco-Tejada, "Progress on the development of an integrated canopy fluorescence model," in *Proc. IGARSS*, vol. 1, Toulouse, France, 2003, pp. 601–603.

[10] R. Peña, A. Ruiz, and J. A. Domínguez, "CEDEX proposal for CHRIS/PROBA activities in 2004 on validation of MERIS models," presented at the *2nd CHRIS/PROBA Workshop*, Frascati, Italy, Apr. 2004.